

Calibrationless Parallel MRI Reconstruction by Using Joint Sparsity Feature

Jiaquan Jin¹, Hongwei Du¹⁺, Bensheng Qiu¹ and Jinzhang Xu²

¹ Center for Biomedical Imaging of University of Science and Technology of China

² School of Electrical Engineering and Automation, Hefei University of Technology

Abstract. In parallel magnetic resonance imaging (pMRI), images between different coils have the similar location of the singularities or discontinuities. As sparsifying transform captures the discontinuities in the images and can be assumed not to affect the position of the discontinuities in the coil images, the corresponding transform results of images from multi-coils can be considered as joint sparse. But previous methods do not consider the property for MRI reconstruction when they include both wavelet transform and total variation. In this paper, we propose a new method based on fast iterative shrinkage/thresholding algorithm (FISTA) and split Bregman algorithm to reconstruct multi-coils images, in which it contains both the joint wavelet sparsity (JWS) and the joint total variation (JTV) regularizers. The experimental results of phantom and brain images show that our proposed algorithm performs better than the other state-of-the-art algorithms.

Keywords: compressed sensing (CS), pMRI, JWS, JTV, FISTA, split bregman.

1. Introduction

Magnetic resonance imaging (MRI) has been widely used in clinical diagnosis over the last decades [1-3]. However, the imaging speed is always limited by the physiological factors such as nerve stimulation and the physical conditions like slew-rate constraints. To accelerate the MRI scanning speed, many researchers are seeking for methods to reduce the amount of necessary k-space data of each coil while preserving adequate image quality.

Compressed sensing MRI (CSMRI) [1] and parallel MRI (pMRI) [2, 3] are two advanced techniques that have been widely used to reconstruct MR images when the k-space data are under-sampled. As CSMRI and pMRI can reconstruct images from different ancillary information (image sparseness for CS and channel sensitivities for pMRI), it is desirable to combine these two techniques to improve image quality without increasing the amount of k-space data. In typical pMRI technologies, the authors reconstructed images by adopting sensitivity information of each coil. However, any inconsistency due to motion or small errors in the sensitivity estimation will lead to significant artifacts in the reconstructed images. In recent years, some researchers begin to use compressed sensing instead of estimating the sensitivity information to reconstruct the multi-coil image. In JTVMRI [4], since MR images are often piece-wise smooth, non-zero gradients only appear on the edges. The author assumes that images from different coils have similar gradient information, thereby the gradients are not only sparse but also joint sparse, then the MRI reconstruction problem can be solved by joint total variation (JTV). In CaLMMRI [5], as wavelet transform encodes the discontinuities about images, the coefficients are very small in smooth areas and large in discontinuous areas. The author assumes that the sensitivity profile is smooth, it does not introduce or get rid of any discontinuity. Thus, if the discontinuity occurs in the original MR image, it should exist in the sensitivity encoded image. So the MRI reconstruction process also can be regarded as a joint wavelet sparsity (JWS) reconstruction problem.

⁺ Corresponding author. Tel.: +86 13625510425.
E-mail address: duhw@ustc.edu.cn.

IN this paper, we propose a new method to improve image quality without increasing sampling ratio by applying CSMRI technique to pMRI. Both popular edge preserving (JTV) and sparsity-promoting (JWS) constraints are introduced into the CS-pMRI reconstruction process. The fast iterative shrinkage/thresholding algorithm (FISTA) is employed to solve the reconstruction problem based on operator splitting technique [6] and split Bregman algorithm [7] is used to solve a subproblem arisen in this model. The experimental results of phantom and brain images show that our proposed method can get better image quality than other state-of-the-art methods.

2. Proposed Method

The parallel MR image reconstruction problem can be expressed as the following minimization problem with a linear inequality constraint, in which it contains both JTV and JWS (called JTW):

$$\mathbf{X} = \arg \min_{\mathbf{X}} \left\{ \alpha \|\mathbf{W}^T \mathbf{X}\|_{2,1} + \beta \|\mathbf{X}\|_{JTV} \right\} \quad s.t. \|\mathbf{A}\mathbf{X} - \mathbf{B}\|_2^2 < \varepsilon, \quad (1)$$

where $\mathbf{X} = [\mathbf{x}_1, \dots, \mathbf{x}_L] \in \mathbb{R}^{n \times L}$ represents a set of vectorial form of L coils images; \mathbf{A} denotes the under-sampled Fourier operator and has proved to accord with compressed sensing criteria [2], so this MR image reconstruction process can be solved by using CSMRI; $\mathbf{B} = [\mathbf{b}_1, \dots, \mathbf{b}_L] \in \mathbb{R}^{n \times L}$ is the multi-coil under-sampled k-space data; \mathbf{W}^T is an orthogonal wavelet transform and ε represents the variance of the signal noise; α and β are two positive parameters; $\|\mathbf{X}\|_{2,1} = \sum_{i=1}^n \left(\sum_{c=1}^L \mathbf{X}_{ic}^2 \right)^{1/2}$ represents the summation of the l_2 norm for each row; $\|\mathbf{X}\|_{JTV} = \sum_{i=1}^n \sqrt{\sum_{c=1}^L (\nabla_1 \mathbf{X}_{ic})^2 + (\nabla_2 \mathbf{X}_{ic})^2}$, ∇_1 and ∇_2 are the finite difference operators on the horizontal and vertical coordinates of an image respectively. Both $\|\mathbf{X}\|_{2,1}$ and $\|\mathbf{X}\|_{JTV}$ are $l_{2,1}$ norm, which is convex and non-smooth.

To solve the JTW model mentioned above, we propose an efficient method based on the FISTA and split Bregman algorithm. By exploiting the Bregman distance, the constrained minimization problem in Equation (1) can be expressed as follows:

$$\begin{cases} \mathbf{X}^{k+1} = \arg \min_{\mathbf{X}} \frac{1}{2} \|\mathbf{A}\mathbf{X} - \mathbf{B}^k\|_2^2 + \alpha \|\mathbf{W}^T \mathbf{X}\|_{2,1} + \beta \|\mathbf{X}\|_{JTV} & (2) \\ \mathbf{B}^{k+1} = \mathbf{B}^k + \mathbf{B} - \mathbf{A}\mathbf{X}^{k+1}. & (3) \end{cases}$$

According to the operator splitting technique based on the proximal operator, the minimization problem (2) can be solved by FISTA:

$$\begin{cases} \mathbf{Y} = \mathbf{X}^k - \rho \mathbf{A}^T (\mathbf{A}\mathbf{X}^k - \mathbf{B}^k) & (4) \\ \mathbf{X}^{k+1} = \arg \min_{\mathbf{X}} \alpha \|\mathbf{W}^T \mathbf{X}\|_{2,1} + \beta \|\mathbf{X}\|_{JTV} + \frac{1}{2\rho} \|\mathbf{X} - \mathbf{Y}\|_2^2. & (5) \end{cases}$$

Problem (5) can be further solved by split Bregman algorithm, its split formulation as follows:

$$\begin{aligned} (\mathbf{X}^{k+1}, \mathbf{Z}^{k+1}, \mathbf{D}_1^{k+1}, \mathbf{D}_2^{k+1}) = \arg \min_{\mathbf{X}, \mathbf{Z}, \mathbf{D}_1, \mathbf{D}_2} & \alpha \|\mathbf{Z}\|_{2,1} + \beta \|\mathbf{D}_1, \mathbf{D}_2\|_{2,1} + \frac{1}{2\rho} \|\mathbf{X} - \mathbf{Y}\|_2^2 + \frac{\lambda}{2} \|\mathbf{Z} - \mathbf{W}^T \mathbf{X} - \mathbf{B}_X^k\|_2^2 \\ & + \frac{\gamma}{2} \|\mathbf{D}_1 - \nabla_1 \mathbf{X} - \mathbf{B}_1^k\|_2^2 + \frac{\gamma}{2} \|\mathbf{D}_2 - \nabla_2 \mathbf{X} - \mathbf{B}_2^k\|_2^2, \end{aligned} \quad (6)$$

where $\mathbf{D}_1 = \nabla_1 \mathbf{X}$, $\mathbf{D}_2 = \nabla_2 \mathbf{X}$ and $\mathbf{Z} = \mathbf{W}^T \mathbf{X}$; $\mathbf{B}_X, \mathbf{B}_1, \mathbf{B}_2$ are auxiliary variables. Then each unknown variable can be solved separately.

As X-subproblem is convex and differentiable, it is easy to get optimality conditions for X. By differentiating with respect to X, we have:

$$\left(\frac{1}{\rho} + \lambda + \gamma \mathcal{V}_1^T \nabla_1 + \gamma \mathcal{V}_2^T \nabla_2 \right) \mathbf{X}^{k+1} = \frac{1}{\rho} \mathbf{Y} + \lambda \mathbf{W} (\mathbf{Z}^k - \mathbf{B}_X^k) + \gamma \mathcal{V}_1^T (\mathbf{D}_1^k - \mathbf{B}_1^k) + \gamma \mathcal{V}_2^T (\mathbf{D}_2^k - \mathbf{B}_2^k). \quad (7)$$

As the Z-subproblem is referring to $l_{2,1}$ norm instead of l_1 norm, it can be solved by a shrinkage operator $shrink_2$, which is defined as [8]:

$$\mathit{shrink}_2(x, \delta) = \frac{x}{\|x\|_2} \max\{\|x\|_2 - \delta, 0\}. \quad (8)$$

Then the Z-subproblem can be calculated as:

$$Z^j = \mathit{shrink}_2\left(\left(\mathbf{W}^T \mathbf{X}\right)^{j(k+1)} + \mathbf{B}_X^{j(k)}, \alpha/\lambda\right), \quad j=1, \dots, n, \quad (9)$$

where $\left(\mathbf{W}^T \mathbf{X}\right)^{j(k+1)}$ is the j -th row of $\mathbf{W}^T \mathbf{X}$ in the $(k+1)$ -th iteration.

For the D_1 and D_2 -subproblems, we can solve them like isotropic TV by a generalized shrinkage formula [9]:

$$D_1^{j(k+1)} = \max\left(s^{j(k)} - \frac{\beta}{\gamma}, 0\right) \frac{\nabla_1 \mathbf{X}^{j(k)} + \mathbf{B}_1^{j(k)}}{s^{j(k)}} \quad j=1, \dots, n, \quad (10)$$

$$D_2^{j(k+1)} = \max\left(s^{j(k)} - \frac{\beta}{\gamma}, 0\right) \frac{\nabla_2 \mathbf{X}^{j(k)} + \mathbf{B}_2^{j(k)}}{s^{j(k)}} \quad j=1, \dots, n, \quad (11)$$

where

$$s^{j(k)} = \left(\left| \nabla_1 \mathbf{X}^{j(k)} + \mathbf{B}_1^{j(k)} \right|^2 + \left| \nabla_2 \mathbf{X}^{j(k)} + \mathbf{B}_2^{j(k)} \right|^2 \right)^{1/2}. \quad (12)$$

Now, we present the proposed algorithm for constrained JTW problem in Algorithm 1. In the inner loop, we set J as 1. Step 1 is the calculation of the gradient of $1/2\|\mathbf{A}\mathbf{X} - \mathbf{B}\|_2^2$. Step 2 that applies split Bregman method is summarized, the value of ρ in (6) is set as 1, the stopping criterion is set as 10^{-3} . Step 3 and step 4 are the acceleration steps in FISTA.

Algorithm 1 Proposed algorithm

Input: $\rho=1/L$, $\mathbf{Y}^1 = \mathbf{X}^0 = \mathbf{0}$, $t^1 = 1$, $\mathbf{B}^0 = \mathbf{B}$, $i = 1$

For $i=1$ **to** K **do**

For $j=1$ **to** J **do**

1. \mathbf{Y} is given by (4)
2. \mathbf{X}^j is given by (5) → Solved by split Bregman
3. $t^{j+1} = \left(1 + \sqrt{1 + 4(t^j)^2}\right) / 2$
4. $\mathbf{Y}^{j+1} = \mathbf{X}^j + (t^j - 1)/t^{j+1} (\mathbf{X}^j - \mathbf{X}^{j-1})$

End for

5. \mathbf{B}^i is given by (3)

End for

Input: $\mathbf{X}^0 = \mathbf{Z}^0 = \mathbf{D}_1^0 = \mathbf{D}_2^0 = \mathbf{B}_X^0 = \mathbf{B}_1^0 = \mathbf{B}_2^0$

While $\|\mathbf{X}^k - \mathbf{X}^{k-1}\|_2 / \|\mathbf{X}^k\|_2 \geq 1e-3$ **do**

1. \mathbf{X}^{k+1} is solved by (7)
2. $\mathbf{Z}^{j(k+1)}$ is given by (9)
3. $\mathbf{D}_1^{j(k+1)}, \mathbf{D}_2^{j(k+1)}$ are given by (10), (11) respectively
4. $\mathbf{B}_X^{k+1} = \mathbf{B}_X^k + (\mathbf{W}^T \mathbf{X}^{k+1} - \mathbf{Z}^{k+1})$
5. $\mathbf{B}_1^{k+1} = \mathbf{B}_1^k + (\nabla_1 \mathbf{X}^{k+1} - \mathbf{D}_1^{k+1})$
6. $\mathbf{B}_2^{k+1} = \mathbf{B}_2^k + (\nabla_2 \mathbf{X}^{k+1} - \mathbf{D}_2^{k+1})$

End while

3. Experiments

3.1. Experimental Setup

In the experiments, two sets of MR data (phantom data and brain data) are employed to demonstrate the superiority of our proposed method in parallel MR image reconstruction. The phantom is piecewise smooth and strictly sparse, which includes the directional curves. The k-space data of brain image is acquired from GE MR750 3T scanner with eight channel coils using T1-weighted fast spin echo (FSE) pulse sequence (TR/TE=500/12.9ms, FOV=24cm, 256×256 matrix). The phantom image and brain image are shown in Fig. 1 (a) and Fig. 1 (b) respectively. Gaussian sampling mask in Fig. 1 (c) is implemented to under-sample the k-space data.

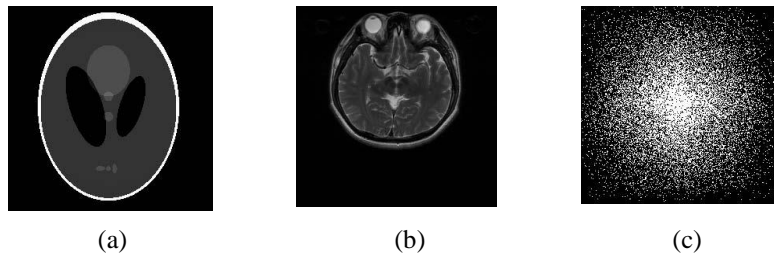


Fig. 1: Original images and Sampling mask, (a) phantom, (b) brain, (c) Gaussian sampling mask.

In the following experiments, we compare our method with the state-of-the-art methods such as CaLMMRI and JTMRI which we mentioned before. For reliability, all codes are downloaded from the authors' websites. In all of the experiments, the white Gaussian noise with 0.01 standard deviation is added in the K-space data to show the robust of the proposed method. The regularization parameters α and β in our algorithm are set as 10^{-2} and 10^{-1} respectively. For comparison, three kinds of image quality measurement tool are used: 1) peak signal-to-noise ratio (PSNR); 2) structural similarity (SSIM); 3) relative error (RE). All experiments were executed, using Windows 7 and MATLAB 2015a (64-bit), on a desktop computer with a 3.2GHz Intel Core i5-4460 CPU and 4GB of RAM.

3.2. Experimental results

The first set of the experiment is about phantom, the reconstructed images by CaLMMRI, JTMRI and the proposed method are presented in Fig. 2 (left part). The Gaussian random sampling ratio is set as 20% and the iteration numbers of these three methods are all set as 100. From the difference images in Fig. 2 (left part), we can see that the main artifacts of the CaLMMRI method locate on the edge parts, the other parts of the reconstructed image get better image quality compared with the edge parts, while the artifacts of the reconstructed image by JTMRI are evenly distributed. Different from CaLMMRI and JTMRI, the proposed method can reconstruct images where the artifacts are not obvious both on edges and on other parts. To make the comparison more intuitive, the reconstruction results at various sampling ratios are presented in Table 1. As the sampling ratio improves, the k-space data contain more information and the image quality (PSNR, SSIM and RE) of the reconstructed image from different methods (CaLMMRI, JTMRI and proposed method) are all improved. When the sampling rate is fixed, the values of PSNR from CaLMMRI are always lower than JTMRI, while the values of SSIM are higher than JTMRI. However, it is exciting that the proposed method inherits the advantages of CaLMMRI and JTMRI, and gets the best image quality.

The second set of experiment is for brain image, the visual reconstructed image results by CaLMMRI, JTMRI and the proposed method are presented in Fig.2 (right part). The Gaussian random sampling ratio is also set as 20% and the iteration number is set as 120. Similarly, the main artifacts caused by the CaLMMRI method focus on edge, and the one in smooth region reconstructed by JTMRI are quite obvious compared with the CaLMMRI method, while the proposed method can reduce the artifacts prominently both in edges and in smooth region since it inherits the advantage of both CaLMMRI and JTMRI. The reconstructed results at various sampling ratios for the brain image are also shown in Table 1. From the value of PSNR and SSIM, we can find that the JTMRI performs better than CaLMMRI when the sampling ratio is high, and when the sampling ratio is very low, such as 18%, the performance of them on the contrary, while the proposed method always performs best no matter the sampling rate is high or low. In a word, compared with the other methods, the proposed method shows better image reconstruction results in both smoothly varying regions and sharp edges.

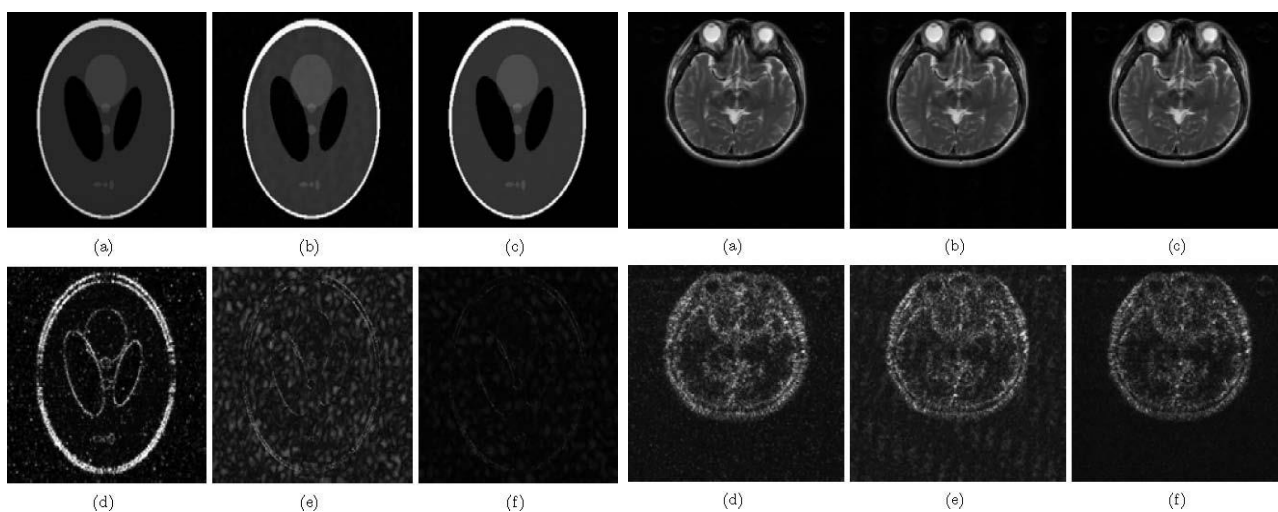


Fig. 2: Reconstructed results of phantom image (left part) and brain image (right part) using Gaussian sampling mask. (a-c) are the reconstructed images by CaLMMRI, JTMRI and the proposed method respectively, (d-f) are the corresponding difference images.

4. Conclusion

In this paper, inspired by the property that MR images from different coils are joint sparse not only in the wavelet transform domain but also in the gradient domain, we put forward a novel MRI reconstruction model that contains both JWS and JTV. To solve this model efficiently, we first translate the constrained problem into a series of unconstrained problems by adopting the Bregman iteration technique. Then FISTA is applied to solve and accelerate the unconstrained problems. Finally, we adopt the split Bregman algorithm to solve the denoising problem which contains the combination of JWS and JTV regularization terms. The experimental results demonstrate that our proposed method can reconstruct the MR images from highly under-sampled k-space data faithfully and outperforms the other two state-of-the-art methods obviously. The proposed method is expected to replace the traditional parallel imaging algorithm which adopting sensitivity estimation. In the future, we will make further efforts to reduce the complexity of the proposed method.

TABLE I: RECONSTRUCTION RESULTS FOR PHANTOM AND BRAIN IMAGES WITH DIFFERENT GAUSSIAN RANDOM SAMPLING RATIOS

Sampling ratio	method	pSNR(dB)	SSIM	RE(%)
		phantom/brain	phantom/brain	phantom/brain
18%	CaLMMRI	36.19/41.41	0.84/0.948	9.51/8.33
	JVMRI	36.43/38.73	0.54/0.829	9.25/11.34
	proposed	43.69/42.56	0.89/0.956	4.01/7.30
20%	CaLMMRI	38.06/42.35	0.88/0.962	7.67/7.48
	JVMRI	44.61/42.35	0.68/0.946	3.60/7.48
	proposed	55.20/44.34	0.94/0.973	1.07/5.95
25%	CaLMMRI	41.96/44.06	0.94/0.971	4.89/6.14
	JVMRI	48.39/44.29	0.77/0.971	2.33/5.98
	proposed	60.80/46.01	0.99/0.980	0.56/4.91
27%	CaLMMRI	44.00/44.62	0.96/0.973	3.87/5.76
	JVMRI	49.66/44.90	0.80/0.974	2.02/5.58
	proposed	62.83/46.66	0.99/0.982	0.44/4.55

5. Acknowledgments

This work was supported by National Natural Science Foundation of China under Grant No.81527802. The authors would like to thank the two healthy volunteers from whom obtained the original MR datasets.

6. References

- [1] M. Lustig, D. Donoho, and J. M. Pauly, "Sparse MRI: The application of compressed sensing for rapid MR imaging," *Magnetic resonance in medicine*, vol. 58, pp. 1182-1195, 2007.
- [2] M. A. Griswold, M. Blaimer, F. Breuer, R. M. Heidemann, M. Mueller, and P. M. Jakob, "Parallel magnetic resonance imaging using the GRAPPA operator formalism," *Magnetic resonance in medicine*, vol. 54, pp. 1553-1556, 2005.
- [3] M. Lustig and J. M. Pauly, "SPIRiT: Iterative self-consistent parallel imaging reconstruction from arbitrary k-space," *Magnetic resonance in medicine*, vol. 64, pp. 457-471, 2010.
- [4] C. Chen, Y. Li, and J. Huang, "Calibrationless parallel MRI with joint total variation regularization," in *International Conference on Medical Image Computing and Computer-Assisted Intervention*, 2013, pp. 106-114.
- [5] A. Majumdar, K. N. Chaudhury, and R. Ward, "Calibrationless parallel magnetic resonance imaging: a joint sparsity model," *Sensors*, vol. 13, pp. 16714-16735, 2013.
- [6] A. Beck and M. Teboulle, "A fast iterative shrinkage-thresholding algorithm for linear inverse problems," *SIAM journal on imaging sciences*, vol. 2, pp. 183-202, 2009.
- [7] J. Duan, Y. Liu, and L. Zhang, "Bregman iteration based efficient algorithm for MR image reconstruction from undersampled k-space data," *IEEE Signal Processing Letters*, vol. 20, pp. 831-834, 2013.
- [8] W. Guo, J. Qin, and W. Yin, "A new detail-preserving regularization scheme," *SIAM journal on imaging sciences*, vol. 7, pp. 1309-1334, 2014.
- [9] T. Goldstein and S. Osher, "The split Bregman method for L1-regularized problems," *SIAM journal on imaging sciences*, vol. 2, pp. 323-343, 2009.